Draft version July 13, 2015
Preprint typeset using LaTeX style emulateapj v. 11/10/09

.

C/O IN PROTOPLANETARY DISKS: THE EFFECT OF RADIAL DRIFT AND VISCOUS ACCRETION

Ana-Maria A. Piso[1], et al

Draft version July 13, 2015

ABSTRACT

...

1. INTRODUCTION

Main sequence stars commonly host giant planets (refs). The chemical composition of gas giant atmospheres can provide important constraints on their formation, accretion and migration history. In recent years, the onset and development of sensitive infrared and (sub)millimeter spectroscopic observations has facilitated the detection of organic molecules in the outer regions of protoplanetary disks (e.g., Öberg et al. 2010, Öberg et al. 2011c, Öberg et al. 2011b, ...). Of particular importance are volatile compounds, since the location of their snowlines determines their relative abundance in gaseous and solid form in the protoplanetary disk, and thus the chemical composition of nascent giant planets.

Notably, an important signature of giant planets atmospheric chemistry is the carbon to oxygen (C/O) ratio. Spectroscopic observations of gas giants such as WASP-12b have found atmospheric C/O ratios close to unity, substantially different from the Solar value of 0.54 (Madhusudhan et al. 2011). One explanation for this discrepancy was proposed by Öberg et al. (2011a), who considered the fact that the main carries of carbon and oxygen, i.e. H_2O, CO_2 and CO, have different condensation temperatures. This changes the relative abundance of C and O in gaseous and solid form as a function of the snowline location of the volatiles mentioned above. Öberg et al. (2011a) calculated analytically the C/O ratio in gas in dust as a function of semimajor axis for passive protoplanetary disks and reproduced a gas C/O ratio of order unity between the CO_2 and CO snowlines, where oxygen gas is highly depleted.

In order to obtain more realistic estimates for C/O ratios across protoplanetary disks, dynamical processes and the disk evolving chemistry have to be taken into account. In this paper, we enhance the model of Öberg et al. (2011a) considering two additional dynamic effects: (1) the radial drift of solids throughout the protoplanetary disk, and (2) the viscous accretion of the disk gas onto the host star. Our goal is two-fold: (1) to quantify the effect of radial drift of solids of different sizes on the location and shape of H_2O, CO_2 and CO snowlines, and (2) to calculate the resulting C/O ratio in gaseous and solid form throughout an actively accreting protoplanetary disk as a function of the grain size distribution and the evolutionary time of the nebula.

This paper is organized as follows: *(section summaries)*.

[1] Harvard-Smithsonian Center for Astrophysics, 60 Garden Street, Cambridge, MA 02138

2. MODEL ASSUMPTIONS

We present our protoplanetary disk model for both a passive and an active disk in section 2.1. In section 2.2, we describe our analytic model for the radial drift of solids. We summarize our ice desorption model in section 2.3. Finally, we discuss the relevant timescales for dynamical effects in the desorption process in section 2.4.

2.1. *Disk Model*

Passive disk. We adopt a minimum mass solar nebula (MMSN) disk model for a passive disk similar to the prescription of Chiang & Youdin (2010). The gas surface density and midplane temperature are

$$\Sigma_{\rm d} = 2200\,(r/{\rm AU})^{-1}\ {\rm g\ cm^{-2}} \quad (1a)$$

$$T_{\rm d} = 120\,(r/{\rm AU})^{-3/7}\ {\rm K}, \quad (1b)$$

where r is the semimajor axis. Based on some observations of protoplanetary disks (Andrews et al. 2010), our surface density profile, $\Sigma_{\rm d} \propto r^{-1}$, is flatter than that of Chiang & Youdin (2010), i.e. $\Sigma_{\rm d} \propto r^{-3/2}$.

Actively accreting disk with passive temperature profile. We model the active disk as a thin disk with an α-viscosity prescription (Shakura & Sunyaev 1973):

$$\nu = \alpha c_{\rm d} H_{\rm d}. \quad (2)$$

Here ν is the kinematic viscosity, $\alpha < 1$ is a dimensionless coefficient and we choose $\alpha = 0.01$, and $c_{\rm d}$, $H_{\rm d}$ are the isothermal sound speed and disk scale height, respectively:

$$c_{\rm d} = \sqrt{\frac{k_{\rm B} T_{\rm d}}{\mu m_{\rm p}}} \quad (3a)$$

$$H_{\rm d} = \frac{c_{\rm d}}{\Omega_{\rm k}}, \quad (3b)$$

where $k_{\rm B}$ is the Boltzmann constant, μ is the mean molecular weight of the gas, $m_{\rm p}$ is the proton mass, and $\Omega_{\rm k}$ is the Keplerian angular velocity, $\Omega_{\rm k} \equiv \sqrt{GM_*/r^3}$, with G the gravitational constant and M_* the stellar mass. We choose $M_* = M_\odot$ and $\mu = 2.35$, corresponding to the Solar composition go hydrogen and helium. The temperature profile for an active disk is assumed to be the same as for the passive disk and given by Equation (1b). From Equations (2) and (3), the viscosity can thus be expressed as a power-law in radius, $\nu \propto r^\gamma$, with $\gamma = 15/14 \approx 1$ for our choice of parameters. Following Armitage (2010), we define $R \equiv r/r_{\rm c}$ and $\nu_{\rm c} \equiv \nu(r_{\rm c})$, where $r_{\rm c}$ is a characteristic disk radius.

We choose $r_c = 100$ AU. The gas surface density is then given by the self-similar solution

$$\Sigma_d(R,T) = \frac{M_d}{2\pi r_c^2 R^\gamma} T^{(-5/2-\gamma)/(2-\gamma)} \exp\Big[-\frac{R^{-(2-\gamma)}}{T}\Big], \quad (4)$$

where M_d is the total disk mass and

$$T \equiv \frac{t}{t_c} + 1 \quad (5a)$$

$$t_c \equiv \frac{1}{3(2-\gamma)} \frac{r_c^2}{\nu_c}, \quad (5b)$$

where t is time. We take $M_d = 0.1 M_\odot$ (e.g., Birnstiel et al. 2012), but note that our results are insensitive to this choice (see Section 5).

Active disk steady-state solution. Calculating the midplane temperature self-consistently for an active disk is non-trivial, so instead we use the steady state solution for the surface density and temperature for a thin disk (e.g., Armitage 2010):

$$T_d^4 = \frac{3GM_*\dot{M}}{8\pi\sigma r^3} \quad (6a)$$

$$\dot{M} = 3\pi\nu\Sigma_d, \quad (6b)$$

where $\dot{M}$, the mass flux, is constant for steady-state [2]. Based on disk observations (e.g., Andrews et al. 2010), we choose $\dot{M} = 10^{-8} M_\odot$ yr^{-1}. We can then easily determine the radial temperature profile from Equation (6a), c_d and H_d from Equation (3), as well as the viscosity ν from Equation (2) for a given α. For consistency, we choose $\alpha = 0.01$ as in the previous case. Finally, we determine Σ_d from Equation (6b).

Static disk. For comparison purposes with Öberg et al. (2011a), we also use a static disk model, with Σ_d and T_d described by Equations (1a) and (1b). The static model does not take into account gas accretion on to the central star or radial drift of solids (see Section 2.2).

2.2. *Radial Drift*

Solid particles in a disk orbit their host star at the Keplerian velocity $v_k \equiv \Omega_k r$. The gas, however, experiences an additional pressure gradient, which causes it to rotate at sub-Keplerian velocity (Weidenschilling 1977). Dust grains thus experience a headwind, which removes angular momentum, causing the solids to spiral inwards and fall onto the host star. Small particles are well-coupled to the gas, while large planetesimals are decoupled from the gas. From Chiang & Youdin (2010), the extent of coupling is quantified by the dimensionless stopping time, $\tau_s \equiv \Omega_k t_s$, where t_s is

$$t_s = \begin{cases} \rho_s s/(\rho_d c_d), & s < 9\lambda/4 \quad \text{Epstein drag} \\ 4\rho_s s^2/(9\rho_d c_d \lambda), & s < 9\lambda/4,\ \mathrm{Re} \lesssim 1 \quad \text{Stokes drag.} \end{cases} \quad (7)$$

Here ρ_d is the gas midplane density, $\rho_s = 2$ g cm^{-3} is the density of a solid particle, s is the particle size, λ is the mean free path, and Re is the Reynolds number.

[2] Equations (6a) and (6b) are valid when $r \gg R_*$, the stellar radius, which is the regime in which we conduct our study.

For a passive disk, the radial drift velocity can be approximated analytically as

$$\dot{r} \approx -2\eta\Omega_k r\Big(\frac{\tau_s}{1+\tau_s^2}\Big), \quad (8)$$

where

$$\eta \equiv -\frac{\partial P_d/\partial \ln r}{2\rho_d v_k^2} \approx \frac{c_d^2}{2v_k^2} \quad (9)$$

and $P_d = \rho_d c_d^2$ is the disk midplane pressure.

For an active disk, the radial drift velocity has an additional term due to the radial movement of the gas, i.e.

$$\dot{r} \approx -2\eta\Omega_k r\Big(\frac{\tau_s}{1+\tau_s^2}\Big) + \frac{\dot{r}_{gas}}{1+\tau_s^2}, \quad (10)$$

where $\dot{r}_{gas}$ is the radial gas accretion velocity and can be expressed as (e.g., Frank et al. 2002)

$$\dot{r}_{gas} = -\frac{3}{\Sigma_d\sqrt{r}} \frac{\partial}{\partial r}(\nu\Sigma_d\sqrt{r}) \quad (11)$$

with Σ_d from Equation (4). For the active disk steady-state solution (see Section 2.1), $\dot{r}_{gas}$ can be expressed more simply using the definition of the mass flux, $\dot{M} = -2\pi r \dot{r}_{gas}\Sigma_d$, with $\dot{M}$ fixed and Σ_d obtained from Equation (6b).

2.3. *Volatile Desorption*

In order for a volatile species to thermally desorb, it has to overcome the binding energy that keeps it on the grain surface. Following Hollenbach et al. (2009), the desorption rate per molecule for a species x can be expressed as

$$R_{des,x} = \nu_x \exp(-E_x/T_{grain}), \quad (12)$$

where E_x is the adsorption binding energy, T_{grain} is the grain temperature, and $\nu_x = 1.6 \times 10^{11}\sqrt{(E_x/\mu_x)}$ is the molecule's vibrational frequency, with μ_x the mean molecular weight. We assume that the dust and gas have the same temperature in the disk midplane, hence $T_{grain} = T_d$. For H_2O, CO_2 and CO, the binding energies E_x are assumed to be 5800 K, 2000 K and 850 K, respectively (Öberg et al. 2011a). We use the desorption rate, R_{des}, to estimate the desorption timescale for particles of different sizes as described in section 2.4.

2.4. *Relevant Timescales*

We can estimate the extent to which radial drift and gas accretion affect desorption by comparing the timescales for desorption, drift and accretion, for solids of different sizes and compositions.

Desorption timescale. We assume that the solid bodies are perfect spheres and are entirely composed of only one volatile species, i.e. either H_2O, CO_2 or CO [3]. The desorption timescale can then be estimated as

$$t_{des} = \frac{\rho_s}{3\mu_x m_p} \frac{s}{N_x R_{des,x}}, \quad (13)$$

where $N_x \approx 10^{15}$ sites cm^{-2} is the number of adsorption sites of volatile x per cm^2 (Hollenbach et al. 2009).

[3] We discuss the validity of these simplifications in section 5.

Radial drift timescale. To order of magnitude, the radial drift timescale can be estimated as

$$t_{\rm r,drift} \sim \frac{r}{\dot{r}}, \tag{14}$$

where $\dot{r}$ is the radial drift velocity given by Equation (8) for a passive disk and by Equation (10) for an active disk.

Gas accretion timescale. The timescale for gas accretion onto the central star for an active disk is (e.g., Armitage 2010)

$$t_{\rm gas,acc} \sim \frac{r^2}{\nu} \sim \frac{1}{2\alpha\eta\Omega_{\rm k}}, \tag{15}$$

with the latter expression derived from Equations (2) and (9).

For simplicity purposes, we calculate the radial drift timescale, $t_{\rm r,drift}$, for a passive disk in this section, but most of our conclusions hold true for an active disk as well. Figure 1 shows $t_{\rm des}$, $t_{\rm r,drift}$ and $t_{\rm gas,acc}$ as a function of particle size at three different locations in the disk, corresponding to the H_2O, CO_2 and CO snowlines in the static disk. As expected, micron-sized particles desorb on very short timescales of $\sim 1-1000$ years in the close vicinity of their respective snowlines, since the desorption rate depends exponentially on temperature and hence disk location (see Equation 12). On the other hand, their radial drift timescale exceeds the typical disk lifetime of a few Myr by several orders of magnitude due to their strong coupling with the gas. Thus for small particles in a passive disk, the snowline locations and the C/O ratio are the same as for a static disk (see Figure 1 from Öberg et al. 2011a) [4]. At the other extreme, kilometer-sized particles are unaffected by gas drag and have long desorption timescales ($\gg$1 Myr), and the snowline locations and C/O ratio remain unchanged in this case as well. This is true for both passive and active disks, since large planetesimals are decoupled from the gas and hence unaffected by gas accretion onto the host star.

Of particular interest for our purposes is the particle size regime for which $t_{\rm r,drift} \lesssim t_{\rm des} \lesssim t_{\rm d}$ or $t_{\rm gas,acc} \lesssim t_{\rm des} \lesssim t_{\rm d}$, where $t_{\rm d} = 3$ Myr is the disk lifetime. In these cases, radial drift or gas accretion (or both) are faster than thermal desorption. Particles of sizes that satisfy these requirements will drift significantly due to radial drift or gas accretion before desorbing, thus moving the H_2O, CO_2 and CO snowlines closer towards the central star and changing the C/O ratio throughout the disk. We quantify these effects in sections 3 and 4.

3. SNOWLINE LOCATIONS

In this section we use the model described in section 2 to quantify the effects of radial drift (passive disk) or radial drift and gas accretion (active disk) on the snowline location, for dust particles of different sizes composed of either H_2O, CO_2 or CO. Specifically, we determine a particle's final location (i.e., where the particle either fully desorbs or remains at its initial size due to a long desorption timescale) as a function of its initial position in the disk, after the gas disk has dissipated. The disk lifetime, $t_{\rm d}$, is particularly relevant since this is the timescale

[4] This is not true for an active disk, however, where gas accretion causes even micron-sized particles to drift significantly before desorbing, as we show in section 3.

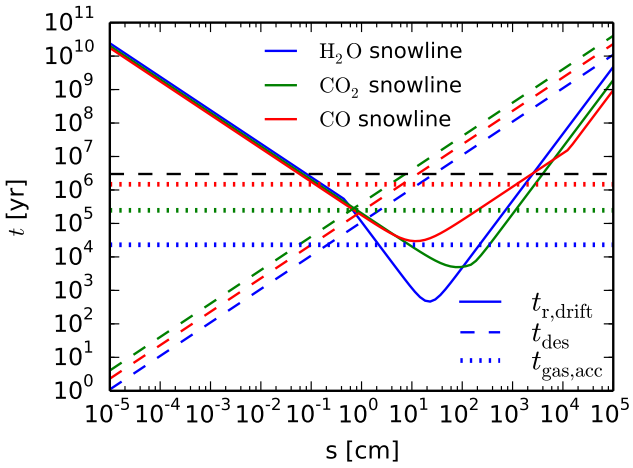

FIG. 1.— Relevant timescales for dynamical effects in the desorption process: $t_{\rm r,drift}$ (solid lines), $t_{\rm evap}$ (dashed lines) and $t_{\rm gas,acc}$ (dotted lines). The timescales are calculated at three representative locations in the disk, i.e. the H_2O, CO_2 and CO snowlines. For our choice of parameters, the snowlines are located at ∼0.7 AU (blue lines), ∼8.6 AU (green lines) and ∼59 AU (red lines), respectively. The horizontal dashed line represents a typical disk lifetime of 3 Myr. Radial drift and gas accretion affect desorption in the regions where their respective timescales, i.e. $t_{\rm r,drift}$ and $t_{\rm gas,acc}$, are comparable to the desorption timescale $t_{\rm des}$.

on which giant planets form. The snowline locations at $t = t_{\rm d}$ throughout the protoplanetary disk determine the disk C/O ratio in gas at this time, and thus the C/O ratio in giant planet atmospheres that have formed *in situ*.

For each species x, we determine the final location in the disk of a particle of initial size s_0 by solving the following system of coupled differential equations:

$$\frac{ds}{dt} = -\frac{3\mu_x m_{\rm p}}{\rho_{\rm s}} N_x R_{\rm des,x} \tag{16a}$$

$$\frac{dr}{dt} = \dot{r}, \tag{16b}$$

where the desorption rate $R_{\rm des,x}$ for each particle type (i.e., composed of H_2O, CO_2 or CO) is evaluated at $T = T_{\rm d}(r)$, and the radial drift velocity $\dot{r}$ is given by Equation (8) for a passive disk and Equation (10) for an active disk. Equations (16a) and (16b) describe the coupled desorption and radial drift, and can be derived straightforwardly from Equation (13). Our boundary conditions are $s(t_0) = s_0$, $r(t_0) = r_0$, and $s(t_{\rm d}) = 0$, where t_0 is the initial time at which we start the integration and r_0 is the initial location of the particle. We choose $t_0 = 1$ year, but our result is independent on the initial integration time as long as $t_0 \ll t_{\rm d}$.

As we show in Section 4, a drifting particle that desorbs will do so almost instantaneously and will lose most of its mass very close to the distance at which it fully desorbs. Thus a particle's final location will depend on whether a grain initially at a certain distance is completely desorbed or not within the disk lifetime of 3 Myr. For example, larger grains take longer to desorb and hence are more likely to not evaporate fully in a given timeframe.

Figure 2 shows our results for H_2O, CO_2 and CO particles, and for both a passive and an active disk. We do

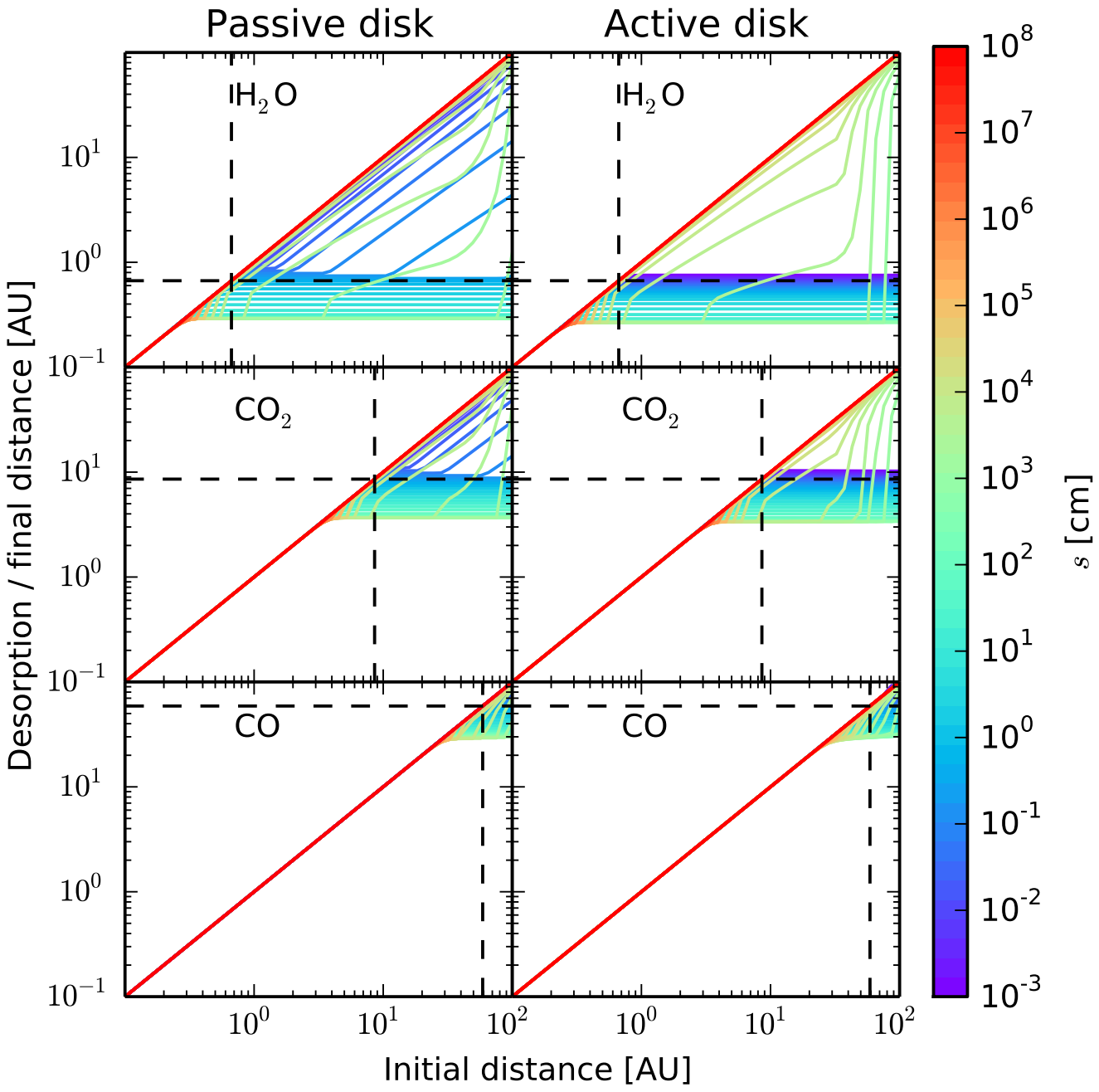

FIG. 2.— Desorption distance as a function of a particle's initial location in the disk, for a range of particle sizes, and for both a passive disk (left panels) and an active disk (right panels). The desorption distance is calculated for particles composed of H_2O (top panels), CO_2 (middle panels) and CO (bottom panels). The particle size increases from 10^{-3} cm to 10^{8} cm as indicated by the color bar. For the range of particle sizes that fully desorb during $t_d = 3$ Myr, the desorption distance is the same regardless of the particles' initial location.

not show the equivalent result for the steady-state active disk since the trends are qualitatively the same as for the active disk with the temperature profile given by Equation (1b). Kilometer-sized bodies do not drift or desorb during the disk lifetime both for a passive and an active disk. Similarly, micron- to mm-sized particles neither drift nor desorb unless they are located inside the static disk snowlines. This is not in contradiction with the desorption timescales for small particles from Figure 1, since small grains only desorb fast at or nearby their respective snowlines, as mentioned in Section 2.4. In an active disk, however, micron-to mm-sized grains do drift significantly since they move at the same velocity as the accreting gas. For 0.5 cm $\lesssim s_0 \lesssim$ 700 cm in a passive disk and 0.001 cm $\lesssim s_0 \lesssim$ 700 cm in an active disk, we notice that particles of initial size s_0 desorb at a fixed distance $r_{\rm des}$ regardless of their original location in the disk. In fact, the only grains that will both drift and evaporate are those that reach their fixed final location (represented by the horizontal curves in Figure 2) within the disk lifetime. We show in section 4 that this result is essential in determining the C/O ratio throughout the disk for different particle sizes.

Intuitively, this fixed $r_{\rm des}$ should be the location in the disk for which $t_{\rm r,drift} \sim t_{\rm des}$, given an initial particle size. Figure 3 shows the validity of this approximation for the range of particle sizes that desorb at a fixed distance in a passive and an active disk. We notice that the analytic approximation accurately reproduces the numerical result for most cases of interest.

4. RESULTS FOR THE C/O RATIO

We now use our model and the results of Section 3 to determine the H_2O, CO_2 and CO snowline locations and the C/O ratio in disks with static chemistry that experience radial drift of solids and gas accretion on to the central star. In Section 3 we showed that solid particles which drift and fully desorb during the lifetime of the protoplanetary disk will do so (1) instantaneously and at (2) at a fixed stellocentric distance, regardless of their initial location in the disk. Figure 5 confirms both of these effects. The left panels show the size evolution with time for H_2O particles of various initial sizes, starting at three different initial locations in a passive disk [5]. Indeed, the solid H_2O particles evaporate almost instantly, although the time $t_{\rm des}$ at which a particle of a given initial size desorbs depends on its initial distance. A particle located at the initial time t_0 at a distance such that $t_{\rm des} > t_{\rm d}$ will therefore not desorb during the disk lifetime. However, our model assumes that particles drift continuously at any location in the disk. Therefore, a particle that can fully desorb during the disk lifetime for at least one initial location will always desorb, at a fixed distance as discussed in Section 3 and displayed in Figure 2. The right panels of Figure 5 show that the drifting grains lose most of their mass in a very narrow distance range; moreover, this distance is the same for a given initial particle size, no matter where the particle started drifting at the time t_0 when the simulation is started. Figure 5 thus proves claims (1) and (2) above. It follows that the H_2O, CO_2 and CO snowlines are fixed for a given initial particle size and disk model (passive or active). The C/O ratio will then only depend on disk properties, grain size, and the abundance of H_2O, CO_2 and CO relative to the H_2 abundance in the disk midplane.

We use the relative number densities of C and O in their different molecular forms (H_2O, CO_2 and CO) from Table 1 of Öberg et al. (2011a). *Is it necessary to reproduce that table? Seems sort of redundant.*. Figure 6 shows the C/O ratio in gas and dust as a function of semimajor axis for a passive disk, an active disk with a passive temperature profile, and a steady-state active disk (not yet there). The C/O ratio for a static disk is shown as a guidline. The plot is consistent with Figure 2. For the passive disk, only grains larger than ∼0.5 cm drift, desorb and thus form a snowline. In contrast, even ∼micron-sized grains drift and desorb for the active disk, since the flow towards the host star together with the accreting gas. For the same particle size, the snowline locations are slightly closer to the central star in the active disk, due to the fact that the accreting gas adds an additional component to the drift velocity of the solids (cf. Equation 10). Perhaps the most interesting feature is the fact that the snowlines are pushed inwards as the grain size increases. While the plot only shows the snowlines and C/O ratio for particle sizes up to ∼7 m, we have found that even kilometer sized boulders are able to drift and desorb for both the passive and the active disk. However, bodies larger than ∼7 m will evaporate at the same location as the meter-sized planetesimals. Thus the innermost snowlines (depicted in red in Figure 6) set the limit on how far close in the H_2O, CO_2 and CO snowlines can be pushed due to radial drift and gas accretion on to the host star. Realistic grain size distributions in disks are dominated by large grains (e.g., D'Alessio et al. 2001, Birnstiel et al. 2012). Therefore, the snowlines produced by the largest drifting solids in our model set the inner limit on the snowline locations and are insensitive to a particular grain size distribution.

5. DISCUSSION AND MODEL LIMITATIONS

5.1. *Dependence on Disk Model and Initial Conditions*

5.2. *Neglected Effects*

Present the diagram that shows all the effects that can modify snowline location. For model limitations, include: non-inclusion of turbulence, assumption of perfect spheres when in fact they may have cracks, particles composed of a single volatile when in reality they are likely to be mixed, etc. Discuss uncertainty of initial conditions and estimate how much they matter. ....

6. SUMMARY AND FUTURE WORK

Summarize results. Mention inclusion of N_2 as a first expansion. Mention the implementation of time-dependent chemical models in the drift calculation.

REFERENCES

[5] Our conclusions remain valid for an active disk and for particles composed of CO_2 or CO.

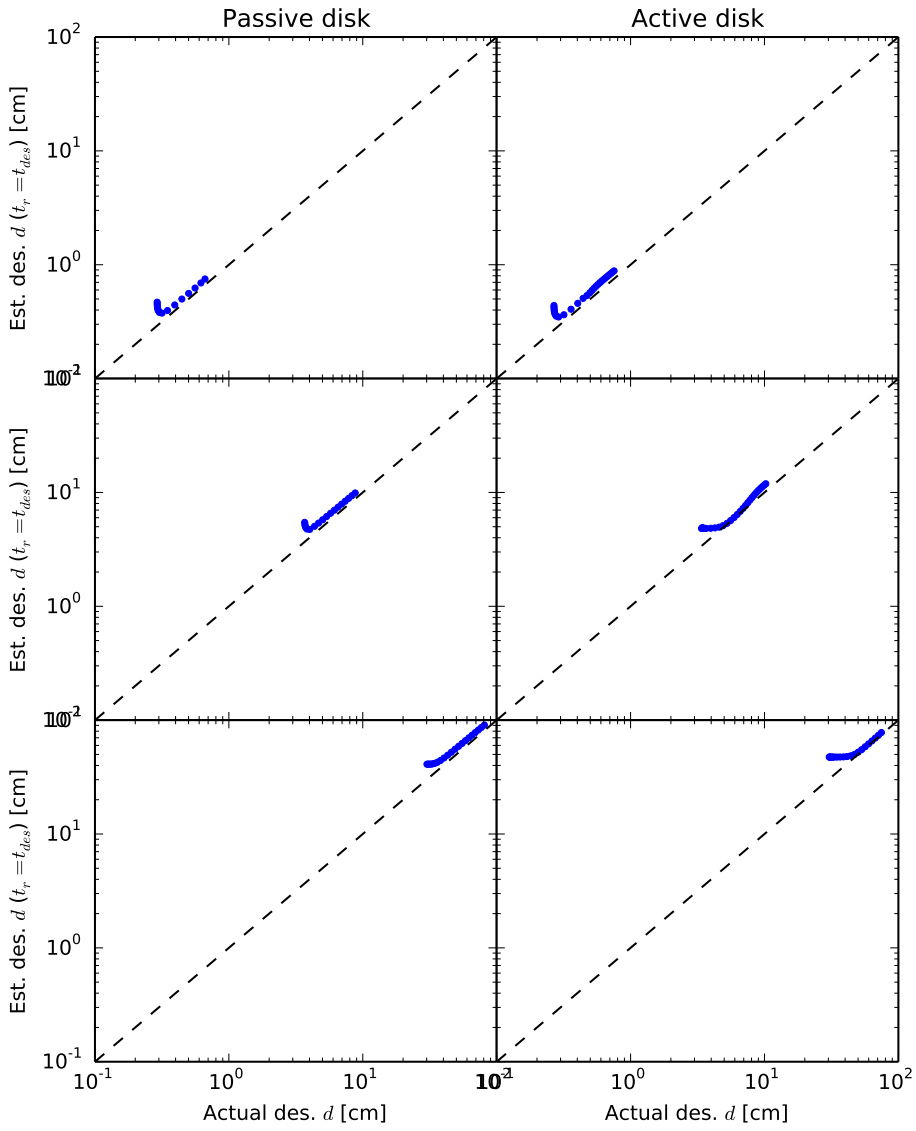

FIG. 3.— Desorption distance estimated from analytic calculations (see text) as a function of the desorption distance calculated numerically, for the range of particle sizes that desorb at a fixed distance regardless of initial location (see Figure 2 and text). The estimate is performed for a passive disk (left panels) and an active disk (right panels). The particles are composed of H_2O (top panels), CO_2 (middle panels) and CO (bottom panels). The analytic approximation is in good agreement with the numerical result for most cases. **Figure belongs to section 3.**

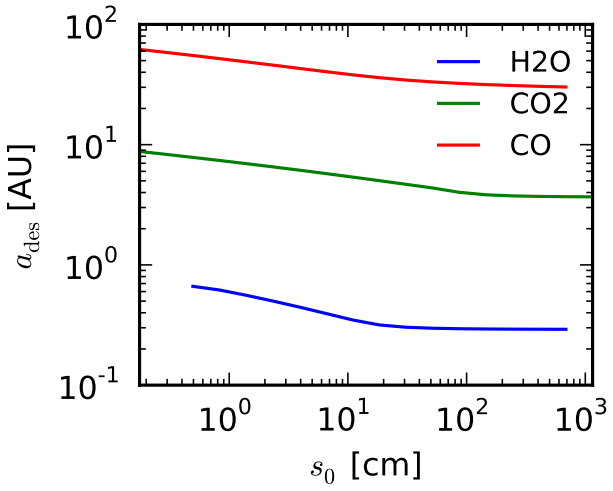

FIG. 4.— Desorption distance as a function of initial particle size, for the range of particles that desorb at a fixed distance regardless of initial location (see Figure 2). **Figure belongs to section 3.** *This is a figure that I'm not sure we should include, since it doesn't really provide that much useful inside. If we did include it though, there would be two panels both for the passive and the active disk. The caption is not complete since the active disk panel is not yet there.*

Andrews, S. M., Wilner, D. J., Hughes, A. M., Qi, C., & Dullemond, C. P. 2010, ApJ, 723, 1241
Armitage, P. J. 2010, Astrophysics of Planet Formation
Birnstiel, T., Klahr, H., & Ercolano, B. 2012, A&A, 539, A148
Chiang, E. & Youdin, A. N. 2010, Annual Review of Earth and Planetary Sciences, 38, 493
D'Alessio, P., Calvet, N., & Hartmann, L. 2001, ApJ, 553, 321
Frank, J., King, A., & Raine, D. J. 2002, Accretion Power in Astrophysics: Third Edition
Hollenbach, D., Kaufman, M. J., Bergin, E. A., & Melnick, G. J. 2009, ApJ, 690, 1497
Madhusudhan, N., Harrington, J., Stevenson, K. B., Nymeyer, S., Campo, C. J., Wheatley, P. J., Deming, D., Blecic, J., Hardy, R. A., Lust, N. B., Anderson, D. R., Collier-Cameron, A., Britt, C. B. T., Bowman, W. C., Hebb, L., Hellier, C., Maxted, P. F. L., Pollacco, D., & West, R. G. 2011, Nature, 469, 64
Öberg, K. I., Murray-Clay, R., & Bergin, E. A. 2011a, ApJ, 743, L16
Öberg, K. I., Qi, C., Fogel, J. K. J., Bergin, E. A., Andrews, S. M., Espaillat, C., van Kempen, T. A., Wilner, D. J., & Pascucci, I. 2010, ApJ, 720, 480
Öberg, K. I., Qi, C., Fogel, J. K. J., Bergin, E. A., Andrews, S. M., Espaillat, C., Wilner, D. J., Pascucci, I., & Kastner, J. H. 2011b, ApJ, 734, 98
Öberg, K. I., Qi, C., Wilner, D. J., & Andrews, S. M. 2011c, ApJ, 743, 152
Shakura, N. I. & Sunyaev, R. A. 1973, A&A, 24, 337
Weidenschilling, S. J. 1977, MNRAS, 180, 57

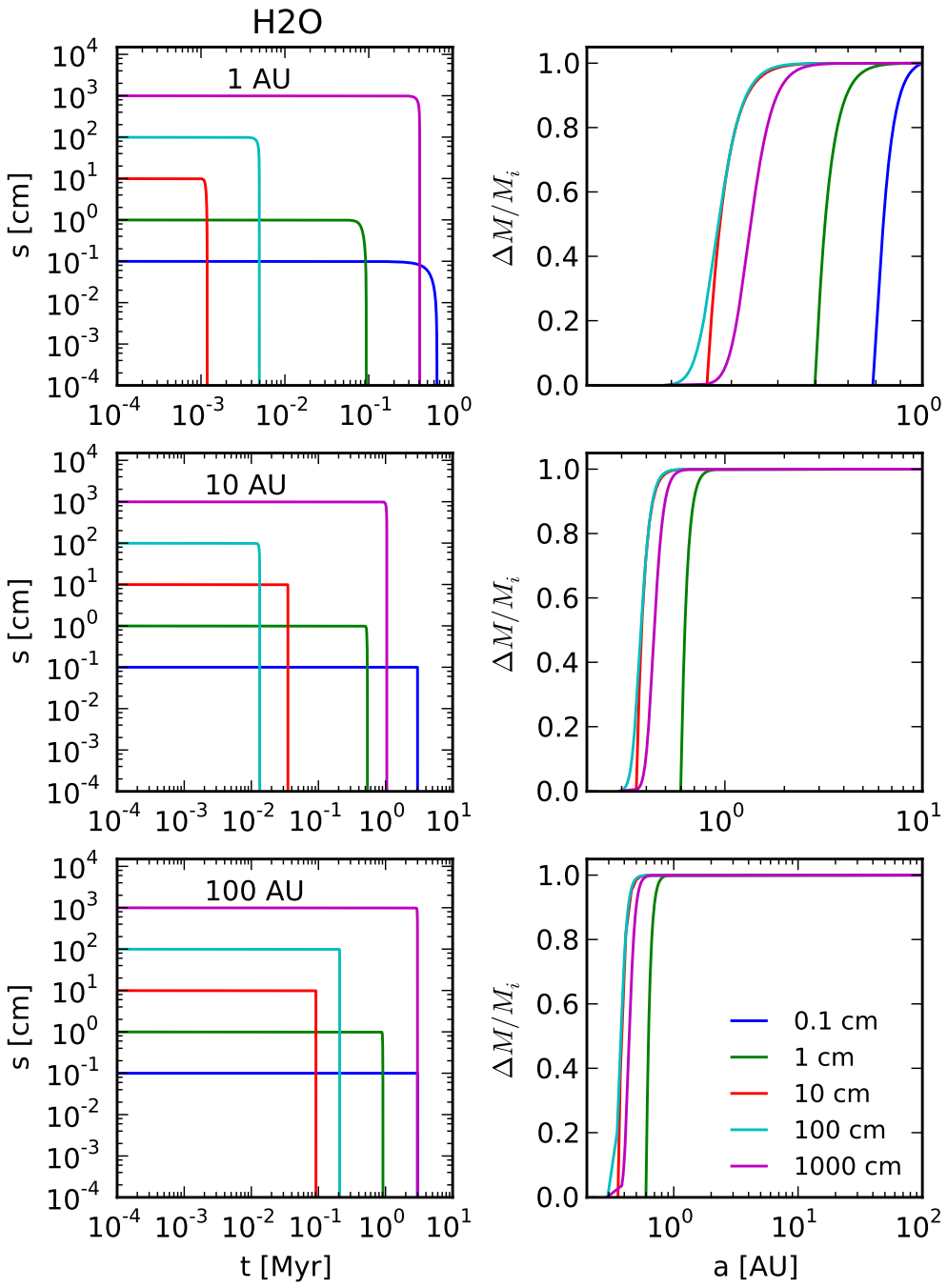

FIG. 5.— Left panels: size of desorbing H_2O particles as a function of time, for different initial particle sizes and for three initial locations in a passive disk: 1 AU (top left), 10 AU (middle left) and 100 AU (bottom left). Particles desorb almost instantaneously. Right panel: fractional mass lost by the desorbing particles as a function of the particle's location as it drifts, for different initial particle sizes, and at the same initial locations presented in the left panel. Particles lose most of their mass very close to the distance at which they fully desorb.

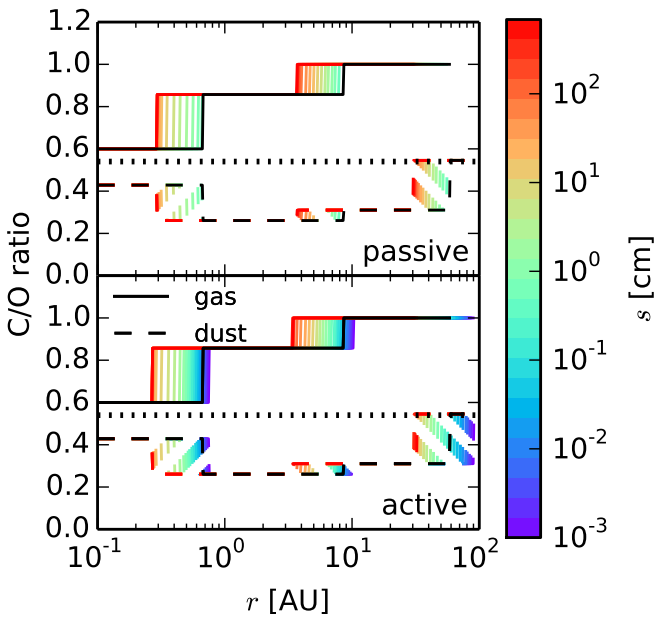

FIG. 6.— C/O ratio in gas (solid lines) and in dust (dashed lines) for a passive disk (top panel) and for an active disk (bottom panel), and for the range of particle sizes that desorb at a fixed distance regardless of their initial location in the disk. The particle size increases from 0.001 cm to ∼700 cm as indicated by the color bar. The horizontal dotted line represents the stellar value of 0.54. The black lines represent the C/O ratio in gas (solid black line) and dust (dashed black line) for a static disk. The snowline location moves inward as the particle size increases. **Figure belongs to section 4.**